Cold-Electron Bolometer Array Integrated with a 350 GHz Cross-Slot Antenna

Mikhail A. Tarasov[1,2,*], Leonid S. Kuzmin[1], Natalia S. Kaurova[1], Ernst A. Otto[1,3], Ghassan Yassin[3], and Paolo de Bernardis[4]

[1]*Chalmers University of Technology, Gothenburg, Sweden*
[2]*Kotel'nikov Institute of Radio Engineering and Electronics of Russian Academy of Sciences, Moscow, Russia*
[3]*Oxford University, Oxford, United Kingdom*
[4] *Rome University, Italy*
*Contact: tarasov@chalmers.se, phone +46-31-7725479

Abstract— **Two series/parallel arrays of Cold-Electron Bolometers (CEB) with Superconductor-Insulator-Normal (SIN) tunnel junctions were integrated in orthogonal ports of a cross-slot antenna. The receiving system was designed for polarisation measurements in a 350 GHz frequency band with JFET readout at the BOOMERanG-FG balloon telescope. Each orthogonal array consists of 10 cold-electron bolometers connected in parallel for RF signal and in series for DC signal. The array was designed to increase the output resistance by a factor of 10^2 in comparison to a single CEB, for matching with JFET readout while maintaining the same conditions for RF coupling. The dynamic resistance of such array is 1 MΩ at the bias point of maximal response. For the input microwave signal bolometers are connected in parallel. This provides matching to the 30 Ω input impedance of a cross-slot antenna on Si substrate. The array of bolometers has a saturation power 10 times higher than a single bolometer. This significantly increases the dynamic range. With a measured temperature response of 8.8 μV/mK, a total absorber volume of 0.08 μm^3, and an output noise of about 11 nV/Hz$^{1/2}$, we estimated the dark electrical noise equivalent power as NEP=6*10^{-18} W/Hz$^{1/2}$ at 280 mK. The optical response was measured using both hot/cold loads and a backward wave oscillator as sources of radiation.**

I. INTRODUCTION

One of the goals is of current Cosmology experiments is to detect the B-mode of the polarization of the Cosmic Microwave Background (CMB), which is believed to be generated by primordial gravitational waves. Several cosmology instruments (e.g. BOOMERanG [1], EBEX, BICEP, QUIET, B-POL) are being designed to measure it. We describe here development of a bolometer system with a JFET readout for the 350 GHz channel of the BOOMERanG-FG balloon telescope.

The optimal detector for this purpose would be the Cold-Electron Bolometer (CEB) based on strong electron cooling of the absorber [2-4]. The concept is based on combination of several functions in a SIN tunnel junction: RF capacitive coupling and effective thermal isolation [3], electron cooling [5], and temperature sensing. The responsivity of a CEB is extremely high, due to the small volume of the absorber and the very low temperature. The CEB can reach remarkable sensitivities of NEP~10^{-19} W/Hz$^{1/2}$ for space-borne telescopes with small optical power load [2]. A high sensitivity of the Cold-Electron Bolometer (CEB) with nanoscale absorber has been observed at 100 mK with a power load of 20 fW; the NEP was below 2*10^{-18} W/Hz$^{1/2}$ [6]. For balloon and ground-based telescopes the CEB sensitivity could be dominated by photon noise of the signal itself, under relatively high optical power loads [7]. We therefore expect that these detectors will be key components for the future European space-mission B-Pol [8], which will follow existing balloon-borne and ground based CMB polarimeters.

At present there are three competing types of incoherent superconducting detectors for space applications. The first and the most developed is the Transition Edge Sensor (TES) [9] with a bias point at the center of the transition of a superconducting strip. The second is the Kinetic Inductance Detector (KID) [10] with a high frequency bias at the resonance frequency. The third is the Cold Electron Bolometer (CEB), with a bias point below the energy gap voltage of a Superconductor-Insulator-Normal metal (SIN) tunnel junction. The CEB is coupled to an antenna through the capacitance of the tunnel junctions, and could be fabricated on planar substrates. CEBs have several advantages over TESs:

- an effective electron cooling of the detector by the readout current for the CEB, in contrast to the heating of the detector by the readout current for the TES. This means that the operating temperature and noise of a CEB are lower than for a TES
- the increased saturation power, due to the ability to remove incoming power from the absorber by effective electron cooling.
- temperature stability is not as important for CEBs as for TESs, because CEBs are based on removing the incoming signal by tunnelling, and the e-ph contribution is rather small.
- the CEB could be matched to MΩ noise impedances of a simple JFET readout (as required by BOOMRanG) in contrast to the TES demanding low-ohmic SQUID readout.

The advantage of CEBs versus TESs is increased when measuring under high background power loads. For example, the dc bias power for a TES should be not less than the maximum signal power, and such bias brings additional thermodynamic noise. The readout for a TES is based on a SQUID amplifier, which is extremely sensitive to external magnetic fields and microphonics. The flexibility of CEBs allows the use of already available readout electronics, based on either semiconductor JFETs, or MOSFETs, or superconducting SQUIDs. In the first case the proper output

matching can be achieved by series array of CEB bolometers [7], that as is described in this paper. For the second case proper output matching can be achieved by using a single CEB with SIN tunnel junction, or a parallel array of CEBs.

II. CEB ARRAY COMPARED TO SINGLE CEB

The CEB concept has been proposed as the main detector for the 350 GHz channel of BOOMERanG [1]. The requirement is to develop a CEB array with a JFET readout for 90 channels. The NEP of the CEB should be less than photon noise for an optical power load of 5 pW, and the cross-polar response should be at least 25 dB below the co-polar one, for observations of CMB and foregrounds polarization. Simulations showed that it is impossible to satisfy these requirements with single CEB plus JFET readout, for both current-biased [7] and voltage biased modes [11]. A novel concept of a series/parallel array of CEBs in current-biased mode has been proposed, offering effective matching to a JFET amplifier under high power load [7] (Fig. 1). The main innovation of the CEB array, in comparison to a single CEB [2-4, 6], is the distribution of power between N CEBs, and the increased dynamic range. An effective distribution of power is achieved by a parallel RF connection of CEBs, which couple to the RF signal through additional capacitances (Fig. 1). The response is increased, because the CEB is sensitive to the level of power, and the power is decreased N times for the individual CEBs, resulting in a proportional decrease of absorber overheating and saturation.

Also the background power is divided among single absorbers, decreasing overheating and increasing the responsivity of the array. The amplifier noise becomes less important, since the responsivity of the array has been multiplied. On the other hand, the increase of the number of bolometers leads to an increase of the absorber volume and corresponding electron-phonon noise. The optimisation of this circuit for a given power load and JFET amplifier is shown in Fig. 2. The optimal number of CEBs is around 10, when total noise is becoming less than photon noise of the incoming signal. This number was used for the design of the device.
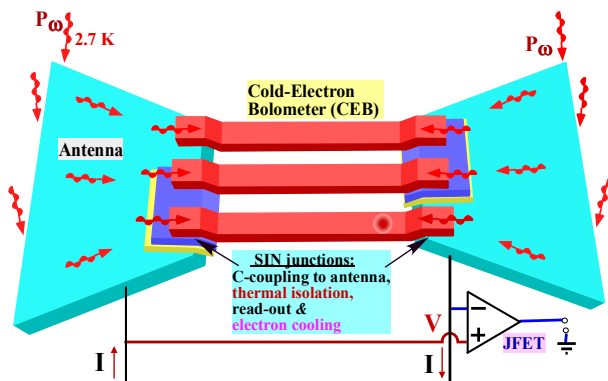

Fig. 2. NEP components and photon NEP versus number of CEBs in the array. The optical power load is Po=5 pW, I_{JFET}=5 fA/Hz$^{1/2}$, V_{JFET}=3 nV/Hz$^{1/2}$, R=1 kΩ, Λ=0.01 μm^3. The responsivity S is also shown to illustrate the effect of CEB number. Thin lines show asymptotics for S and NEP$_{JFET}$ [7].

III. EXPERIMENTAL TECHNIQUE

The layout design of CEB array has been optimized for polarization measurements in a 345 GHz frequency band for CMB and foregrounds polarisation measurements with the balloon-borne telescope BOOMERANG. Bolometers are integrated in a cross-slot antenna that is placed in the centre of a 7x7 mm chip on oxidized Si substrate. Antenna design is similar to [12]. Each orthogonal array consists of 10 CEBs connected in series for dc bias and readout. A picture of the antenna is presented in Fig. 3. The dark narrow slots are covered with an Al capacitive layer. Each port of the antenna contains 5 CEBs that are connected in series for each polarisation, making an array of 10 CEBs for vertical and 10 CEBs for horizontal polarization components. The NIS tunnel junctions of CEBs are made of CrAl/AlOx/Al thrilayer. An advanced shadow-evaporation technique was used for fabrication of the CEB [13]. A detailed SEM view of a half an array with 5 absorbers and 10 tunnel junctions is presented in Fig. 4.

Fig.1. Schematic of an array of three CEBs with series connection for DC bias and parallel connection for RF. This solution was devised to match a JFET readout. For RF signals the CEBs are connected in parallel through the additional capacitances between the superconducting islands and the antenna.
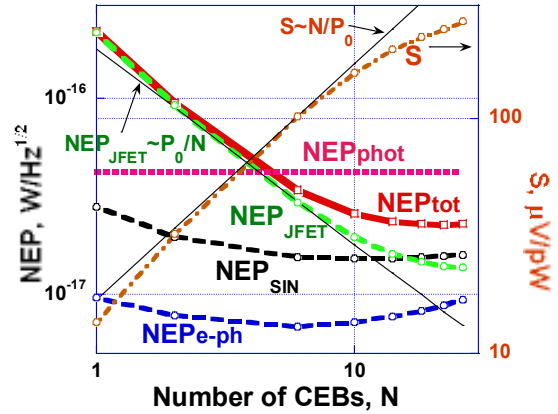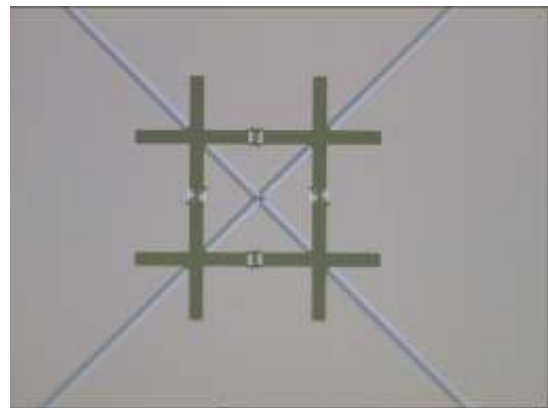

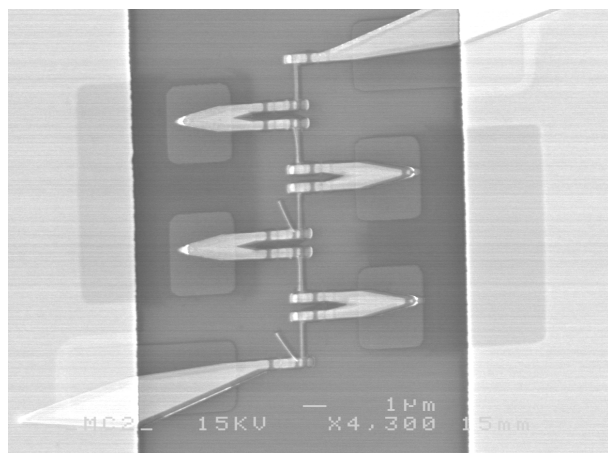Fig. 3. Optical image of a cross-slot antenna.

Fig. 4. SEM image of a half of array consisting of 5 absorbers and 10 SIN tunnel junctions.

Each array was protected against external interferences by four on-chip CrPd resistors with 12 nm Cr and 3 nm Pd [13]. The Pd layer was added to improve contact with the top layer of the bolometer structure. Current lead resistors have a value of 2 MΩ and voltage lead resistors have a value of 150 kΩ each.

Such a chip with antenna is attached to an extended Si lens with antireflection coating, or to the horn antenna for simple measurements with a cold radiation source. The lens is facing the optical window through low-pass filters at two temperature stages, as is shown in Fig. 5 .
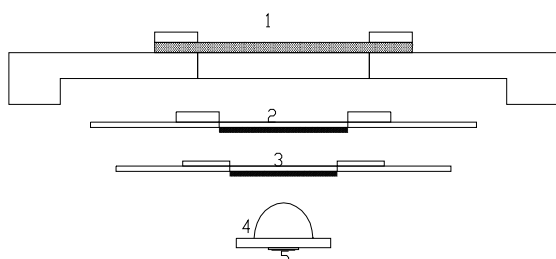

Fig. 5. Schematics of the quasioptical beam path in the cryostat. (1) - Teflon window, (2) - first low-pass filter, (3) - second low-pass filter, (4) – Si extended hyper-hemisphere lens, (5) - sample chip.

To suppress overheating by IR radiation, the optical window is protected by low-pass filters (LPF). Commercial low-pass multi-mesh filters from QMC Instruments™ provide attenuation over 10 dB above the cut-off frequency of 100 cm^{-1} for LPF W97s and above 33 cm^{-1} for LPE B694. Filters were placed at the openings in the radiation shields at the 70 K and 3 K temperature stages. With these filters, however, we measured significant overheating of the cold stage, and reduced holding time for the He3 sorption cooler. Usual low-pass filters for 30 cm^{-1} is array of metal film squares 300 μm sides on thin dielectric support like KAPTON™. Metal squares are radiation heated from the warmer side of cryostat and as a result their equilibrium temperature is some average between hot and cold sides. It

means that such filter is a source of thermal radiation above the cut-off frequency. A band-pass filter consisting of cross-shaped holes in a metal film can be better from the overheating point of view, because it can be anchored thermally very well to the radiation shield, and its equilibrium temperature is the same as the shield. In our case we solved the problem placing neutral density filters (NDF) with attenuation about 6 dB in front of each LPF. As a result IR radiation was suppressed; the temperature of self irradiation is the same as the radiation shield and no visible overheating of the cold stage or reduction of holding time was measured.

IV. MEASUREMENT RESULTS

The IV characteristic of the array of ten SINIS cold-electron bolometers, together with the voltage response to temperature differences are presented in Fig. 6. It clearly demonstrates the sum gap voltage of 20 SIN junctions. The resistance ratio of subgap resistance to normal resistance for this array is over 500, close to the theoretical estimates for a temperature of 280 mK. The voltage at a 0.1 nA bias current together with the dynamic resistance at zero bias versus temperature are presented in Fig. 7. The maximum voltage response to temperature is 8.8 µV/mK.
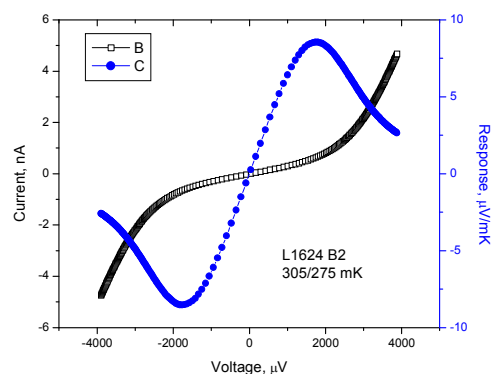

Fig. 6. IV curve and voltage response for a temperature difference of 305-275 mK
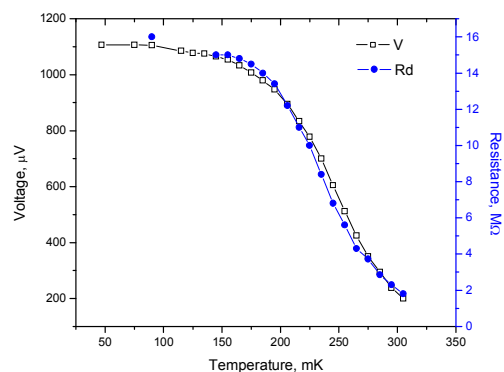

Fig. 7. Voltage across the array of 10 bolometers, for a bias current 0.1 nA, versus temperature of the array. The maximum responsivity is 8.8 µV/mK. Dynamic resistance at zero bias is for comparison.
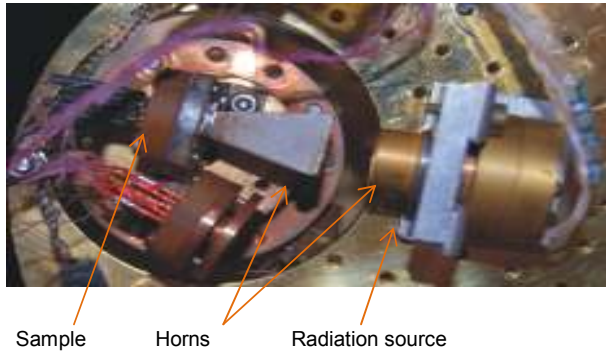
Fig. 8. Bottom view of the open cryostat, with the sample on the 300 mK stage and the radiation source on the 3 K stage
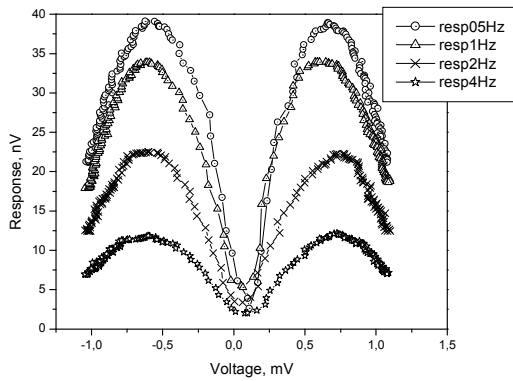

Fig. 9. Voltage response of the bolometer array to radiation emitted from a source modulated at 0.5 Hz, 1 Hz, 2 Hz, 4 Hz, versus dc bias voltage of the array.

Fig. 10. Photo of rotatable aperture with Cu shield at one side and 10 dB NDF at other side. Below is the magnet by which we can precisely rotate the aperture, to place Cu shield, NDF, or OPEN between the bolometer and the window.

We measured the response of this array to microwave radiation emitted by a cryogenic thermal radiation source (Fig. 8, 9). The source was mounted on the 2.8 K stage; it consists of a NiCr film on a thin sapphire substrate, and was attached to a horn directing radiation to the bolometer unit with its own horn at 280 mK. Such source is relatively slow and its modulation depth decreases increasing the modulation frequency, so the measured signal amplitude decreases from 40 nV to 10 nV when the frequency rises from 0.5 Hz to 4 Hz.. The temperature increase of the radiation source is estimated to be about 1 K, so the emitted power in the 100 GHz bandwidth is of the order of 1 pW. Microwave losses due to beam mismatch, reflection from Si substrate back side, mismatch of horns are estimated to be above 30 dB.

For correct optical measurements, and to get an additional calibration of the bolometer input, we installed inside the cryostat a holder with a Cu foil opaque screen, a 10 db NDF, and an open aperture. The holder can be rotated by an external magnet while the experiment is cold. A photo of this setup being tested at room temperature is presented in Fig. 10; the measured signal is shown in Fig. 11.

The measured temperature sensitivity is 17 µV/K and the optical noise equivalent temperature difference is NETD=0.65 mK/Hz$^{1/2}$. Similar response dependencies were measured with hot/cold load at 300/77 K in front of the optical window.

For NEP estimations we measured the output noise of the array using a MOSFET OPA111 instrumentation amplifier as input IC. The corresponding NEP can be calculated from the available data on array parameters. For theoretical estimations of such bolometer array performance we can take the power flow determined only by electron-phonon interaction $P=\Sigma v(T^5-T_0^5)$ so that $G=dP/dT=5\Sigma vT^4$. In this case the responsivity is $S=dV/dP=(dV/dT)/(dT/dP)=(dV/dT)/G$. The volume of the absorber for our array of 10 bolometers is $v=10^{-19}$ m^3 and for aluminium $\Sigma=1.2*10^9$ Wm^{-3}K^{-5}: so the thermal conductivity is $G=3.6*10^{-12}$ W/K at 280 mK phonon temperature. Taking the measured bolometer output voltage noise of $v_n=11$ nV/Hz$^{1/2}$ in the white noise region, and a temperature response of $dV/dT=8.8*10^{-3}$ V/K (see Fig. 6) we can estimate the minimum noise equivalent power $NEP=v_n/S=6*10^{-18}$ W/Hz$^{1/2}$. For practical power load of 5 pW at 345 GHz, the photon contribution to NEP can be estimated as $NEP_{phot}=(2P_0hf)^{1/2}=4.8*10^{-17}$ W/Hz$^{1/2}$. Taking into account the experimental values of noise and response, we can plot the dark NEP of our bolometer array, see Fig. 12, 13.
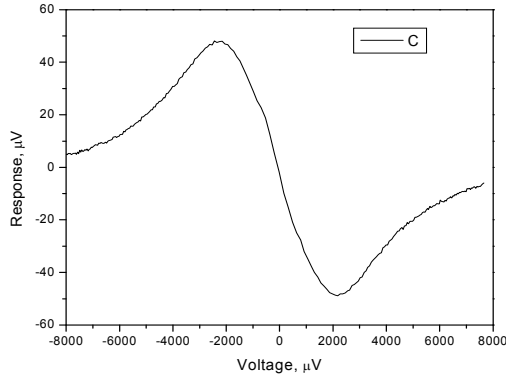
Fig. 11. Voltage response to changing aperture from Cu foil to NDF 10 dB attenuator at 3 K.
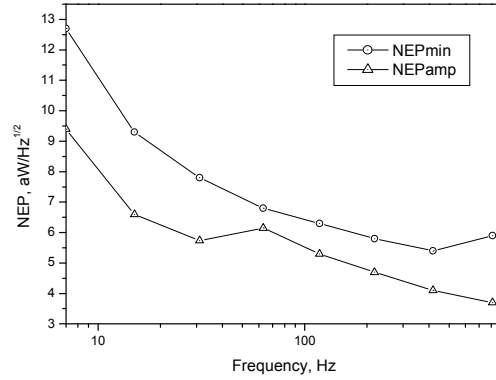

Fig. 13. The minimum Noise Equivalent Power (NEP) from Fig. 14 and the contribution due to the amplifier.
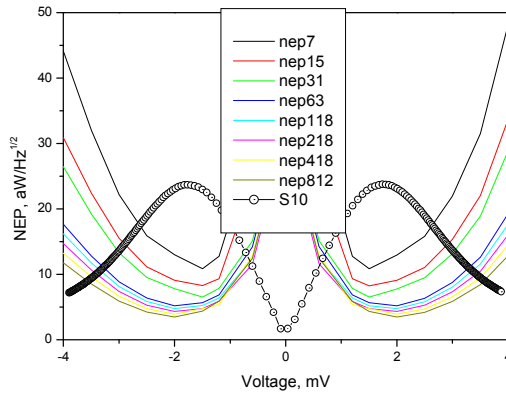

Fig. 12. The Noise Equivalent Power (NEP) and absolute value of response for the series array of 10 bolometers.
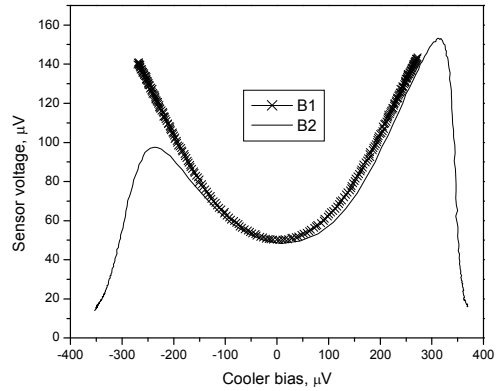

Fig. 14. The electron cooling measured by the voltage across small-area sensor junctions, versus the voltage across the bolometer junctions that serve as electron coolers.

Optical NEP can be also estimated from Fig. 11. The incoming power P_{sig} at the signal frequency f=350 GHz within the bandwidth of the cross-slot antenna Δf=100 GHz is calculated from Planck formula

$$\Delta P = \frac{hf}{\exp(hf/kT)-1}$$

so that $P_{sig}=\Delta P*\Delta f=10^{-13}$ W. The response for this signal is 50 μV so the responsivity is S=dV/dP=5*10^8 V/W. For an output noise of V_n=11 nV/Hz$^{1/2}$ we obtain the total optical NEP=V_n/S=2.2*10^{-17} W/Hz$^{1/2}$.

We also observe the effect of electron cooling. On the same chip we have a test structure comprising a single bolometer of the same shape as in the array and with the absorber connected to another pair of SIN sensor junctions. Applying the bias voltage to the bolometer part we can sense the resulting electron temperature in the absorber. The results of such a measurement are presented in Fig. 14. The maximum increase in sensor voltage is about 105 μV. Taking into account the calibration curve for sensor junctions with dV/dT=1.08 μV/mK one can estimate the cooling effect as 97 mK. So we can expect a maximum cooling of -97 mK at the corresponding bias point of 3 mV, for the series array of 10 bolometers. Maximum response for array is observed at a bias voltage of 2 mV, that corresponds to a 200 μV bias voltage for each single bolometer, like in Fig. 14. At this voltage we have an increase of the sensor voltage by 49 μV, that corresponds to cooling down by 45 mK, i.e. from the base temperature of 276 mK down to 230 mK.

The effectiveness of connecting bolometers in a series array and electron cooling can be illustrated by direct optical measurements of dynamic range. For such experiment we use Backward Wave Oscillator (BWO) that operates in a frequency range of 250-380 GHz for anode voltages in the range 1100-3800 V. A calibrated polarisation grid attenuator was used for accurate control of the incident power. Inside the cryostat besides the 20 dB NDF cold attenuator at the optical window we also use our cold rotatable stage with opaque Cu window, 10 dB NDF, and open aperture. A photo of a room-temperature setup is presented in Fig.15. The measured output voltage dependence on signal attenuation is presented in Fig. 16.

Fig. 15. The backward wave oscillator (to the right), the polarisation grid attenuator (in the center), and the optical window of He3 cryostat (to the left) in the experiment to measure the dynamic range of the bolometer.
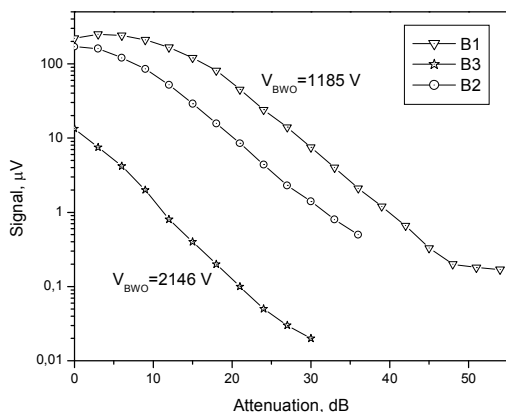

Fig. 16. The output voltage dependence on incoming signal attenuation for 242 GHz and 292 GHz radiation from backward wave oscillator.

Accuracy of such measurements is limited by mechanical instabilities and leak of power through NDF. Nevertheless even in this experiment the dynamic range is over 30 dB. If we take the lower signal level equal to amplifier noise of 11 nV/Hz$^{1/2}$ and saturation level as presented in Fig. 16 of 200 µV both measured with integration time 1 s, this results in a full dynamic range of bolometer array over 43 dB.

V. CONCLUSIONS

Optical response with NEP=V_n/S=2.2*10^{-17} W/Hz$^{1/2}$ at 345 GHz, temperature response dV/dT=8.8 µV/K, power response dV/dP=8.6*10^{8} V/W, optical NETD=0.65 mK/Hz$^{1/2}$; dark NEP=6*10^{-18} W/Hz$^{1/2}$, and dynamic range over 30 dB were measured at T=280 mK for a series array of cold-electron bolometers integrated in a cross-slot antenna. Electron cooling by 45 mK at maximum response bias point improves the NEP of such detector and increases the dynamic range.

REFERENCES

[1] S. Masi et al , "Instrument, Method, Brightness and Polarization Maps from the 2003 flight of BOOMERanG", 2006, *Astronomy and Astrophysics*, 458 , 687-716, astro-ph/0507509

[2] L. Kuzmin, "Ultimate Cold-Electron Bolometer with Strong Electrothermal Feedback", *Proc. of SPIE conference*, vol. 5498, pp 349-361, June 2004.

[3] L. Kuzmin *"On the Concept of a Hot-Electron Microbolometer with Capacitive Coupling to the Antenna"*, *Physica B: Condensed Matter*, vol. 284-288, 2129 (2000).

[4] L. Kuzmin and D. Golubev, "On the concept of an optimal hot-electron bolometer with NIS tunnel junctions" *Physica C, vol.* 372-376, pp 378-382 (2002).

[5] M. Nahum, T. M. Eiles, and J. M. Martinis, "Electronic micrtorefrigerator based on a normal-insulator-superconductor tunnel junction". *Appl. Phys. Lett , vol.* 65, 3123 (1994).

[6] A. Agulo, L. Kuzmin, M. Tarasov, "Attowatt sensitivity of the Cold-Electron Bolometer". Proceedings of the 16th Int. Symp. On Space Terahertz Technol., ISSTT2005, pp 147-152, Gothenburg, Sweden, May 2005.

[7] Leonid Kuzmin, "Array of Cold-Electron Bolometers with SIN Tunnel Junctions for Cosmology Experiments". *Journal of Physics*: Conference Series (JPCS), vol. 97, 012310 (2008).

[8] Leonid Kuzmin, Ghassan Yassin, Stafford Withington, and Paul Grimes. "An Antenna Coupled Cold-Electron Bolometer for High Performance Cosmology Instruments", Proc. of the 18th ISSTT, pp 93-99, Pasadena, March 2007 .

[9] K. Irwin "An application of electrothermal feedback for high-resolution particle detectors". *Applied Physics Letters*, vol. 66, p.1998, (1995).

[10] N. Grossman, D. G. McDonald, and J. E. Sauvageau, "Far-infrared kinetic-inductance detectors". *IEEE Trans. Magn.*, vol. 27, 2677 (1971).

[11] Leonid Kuzmin, "A Superconducting Cold-Electron Bolometer with SIS´ and Josephson Tunnel Junctions", Journal of Low Temperature Physics, **151**, pp. 292-297 (2008).

[12] G.Chattopadhayay, F.Rice, D.Miller, H.G.LeDuc, and J.Zmuidzinas, "A 530-GHz balanced mixer", *IEEE Microwave Guide Wave Lett.*, vol. 9, pp. 467-469 , Nov. 1999.

[13] Leonid Kuzmin. "Self-Aligned Shadow-Evaporation Technology for Large Area Tunnel Junctions and Nanoabsorbers". PCT Patent, to be filed (August 2010).

[14] L.S. Kuzmin, Yu.V. Nazarov, D.B. Haviland, P. Delsing and T. Claeson. "Coulomb Blockade and Incoherent Tunneling of Cooper Pair in Ultra-Small Junctions Affected by strong Quantum Fluctuations", Phys. Rev. Lett. Vol.67, 1161 (1991).

261